AGU PUBLICATIONS

JGR

Journal of Geophysical Research: Oceans

RESEARCH ARTICLE

10.1002/2017JC012839

Special Section:
The Southern Ocean Carbon and Climate Observations and Modeling (SOCCOM) Project: Technologies, Methods, and Early Results

Annual nitrate drawdown observed by SOCCOM profiling floats and the relationship to annual net community production

Kenneth S. Johnson[1], Joshua N. Plant[1], John P. Dunne[2], Lynne D. Talley[3], and Jorge L. Sarmiento[4]

[1]Monterey Bay Aquarium Research Institute, Moss Landing, California, USA, [2]National Oceanic and Atmospheric Administration/Geophysical Fluid Dynamics Laboratory, Princeton, New Jersey, USA, [3]Scripps Institution of Oceanography, University of California, San Diego, La Jolla, California, USA, [4]Program in Atmospheric and Oceanic Sciences, Princeton University, Princeton, New Jersey, USA

Key Points:
- Vertically resolved distributions of nitrate were measured over full annual cycles using optical nitrate sensors on profiling floats
- Annual nitrate drawdown was used to estimate annual net community production throughout the Southern Ocean
- Zonally averaged annual net community production is maximum in the Subantarctic Zone

Correspondence to:
K. S. Johnson,
johnson@mbari.org

Citation:
Johnson, K. S., J. N. Plant, J. P. Dunne, L. D. Talley, and J. L. Sarmiento (2017), Annual nitrate drawdown observed by SOCCOM profiling floats and the relationship to annual net community production, *J. Geophys. Res. Oceans*, *122*, 6668–6683, doi:10.1002/2017JC012839.

Received 27 FEB 2017
Accepted 4 JUL 2017
Accepted article online 26 JUL 2017
Published online 25 AUG 2017

Abstract Annual nitrate cycles have been measured throughout the pelagic waters of the Southern Ocean, including regions with seasonal ice cover and southern hemisphere subtropical zones. Vertically resolved nitrate measurements were made using in situ ultraviolet spectrophotometer (ISUS) and submersible ultraviolet nitrate analyzer (SUNA) optical nitrate sensors deployed on profiling floats. Thirty-one floats returned 40 complete annual cycles. The mean nitrate profile from the month with the highest winter nitrate minus the mean profile from the month with the lowest nitrate yields the annual nitrate drawdown. This quantity was integrated to 200 m depth and converted to carbon using the Redfield ratio to estimate annual net community production (ANCP) throughout the Southern Ocean south of 30°S. A well-defined, zonal mean distribution is found with highest values (3–4 mol C m^{-2} yr^{-1}) from 40 to 50°S. Lowest values are found in the subtropics and in the seasonal ice zone. The area weighted mean was 2.9 mol C m^{-2} yr^{-1} for all regions south of 40°S. Cumulative ANCP south of 50°S is 1.3 Pg C yr^{-1}. This represents about 13% of global ANCP in about 14% of the global ocean area.

Plain Language Summary This manuscript reports on 40 annual cycles of nitrate observed by chemical sensors on SOCCOM profiling floats. The annual drawdown in nitrate concentration by phytoplankton is used to assess the spatial variability of annual net community production in the Southern Ocean. This ANCP is a key component of the global carbon cycle and it exerts an important control on atmospheric carbon dioxide. We show that the results are consistent with our prior understanding of Southern Ocean ANCP, which has required decades of observations to accumulate. The profiling floats now enable annual resolution of this key process. The results also highlight spatial variability in ANCP in the Southern Ocean.

1. Introduction

Organic matter produced in the surface ocean and exported below the euphotic zone (Export Production, EP), places strong constraints on the Earth's climate. This "biological pump" creates a surface depletion in dissolved inorganic carbon that is a major control on atmospheric pCO_2 [*Sarmiento et al.*, 2011]. Atmospheric CO_2 concentration is reduced by about 200 ppm through the biological pump [*Watson and Orr*, 2003; *Parekh et al.*, 2006]. The largest influence of this process occurs in the Southern Ocean [*Marinov et al.*, 2008].

Export production is driven by net community production (NCP) of organic carbon in the euphotic zone. NCP is the balance between primary production of organic matter in the euphotic zone and respiration of that matter by organisms at all trophic levels within the upper ocean [*Emerson*, 2014]. ANCP is the annual integral of NCP. ANCP must be in an approximate balance with the annual organic carbon export (EP) into the deep sea [*Falkowski et al.*, 2003]. Methods of estimating ANCP thus provide tools to understand spatial and temporal variability in EP and the controls on atmospheric CO_2.

Recent surface data have shown that air-sea CO_2 fluxes in the Southern Ocean are more dynamic than once thought [*Landschützer et al.*, 2015]. There is little corresponding information on interannual variations in EP

or ANCP that may impact fluxes. Estimates of the biological pump strength can be measured from below the euphotic zone with sediment traps or respiration of organic carbon (EP), or inferred from above by measuring annual net community production (ANCP). ANCP can be estimated by converting changes in euphotic zone nutrient inventories to changes in carbon inventories assuming they are related by Redfield ratios [*Munro et al*., 2015; *Plant et al*., 2016]. At the scale of an ocean basin or larger, ANCP has been estimated from global climatologies of dissolved inorganic carbon [*Lee*, 2001] and nitrate [*MacCready and Quay*, 2001] and from compilations of sediment trap data [*Dunne et al*., 2007]. However, these estimates include data spanning many decades and do not provide information on seasonal or interannual variability. Direct measurements of ANCP with annual resolution are generally only available at a few ocean time series stations [*Gruber et al*., 1998; *Keeling et al*., 2004; *Emerson*, 2014]. It is not clear how ANCP and EP will change in future oceans [*Riebesell et al*., 2009; *Boyd*, 2015].

The spatial distribution of ANCP also has important implications for atmospheric CO_2. Numerical models show a biochemical divide in the Southern Ocean centered where waters with a potential density anomaly (density, 1000) of 27.3 kg m^{-3} outcrop at the surface (near 50°S) [*Marinov et al*., 2006]. ANCP changes to the south of this divide have large effects on atmospheric CO_2, while changes in ANCP in the Subantarctic waters to the north have a much weaker impact. Unused nutrients in the Subantarctic surface waters are subducted with intermediate waters that flow northward. As a result, increases in Southern Ocean ANCP north of the divide result in a counterbalancing decrease in subtropical ANCP and little net change in atmospheric CO_2. On the other hand, ANCP to the south of the divide removes dissolved inorganic carbon from surface waters and sequesters it in deep waters where it does not rapidly return to the surface.

Thus, it is important to have both long-term and spatially resolved measurements of ANCP throughout the Southern Ocean. Long-term deployments of chemical sensors on profiling floats now provide the ability to estimate ANCP in remote regions of the ocean [*Riser and Johnson*, 2008; *Martz et al*., 2008; *Bushinsky and Emerson*, 2015; *Plant et al*., 2016; *Hennon et al*., 2016]. Measurements of the annual production of oxygen [*Riser and Johnson*, 2008; *Bushinsky and Emerson*, 2015] or depletion of nitrate [*Plant et al*., 2016] using sensors mounted on profiling floats can provide direct estimates of ANCP after the Redfield ratio is used to convert the measured quantity to carbon uptake. While these sensors can be deployed on a variety of other platforms, such as moorings [*Shadwick et al*., 2015] or gliders [*Nicholson et al*., 2008], the high operational costs of these platforms [*Rudnick et al*., 2012] generally preclude large arrays from being deployed [*Rudnick*, 2016]. The Argo program [*Riser et al*., 2016] has demonstrated that very large arrays of profiling floats can be operated at the global scale.

The major focus of this paper is to report the annual cycle in nitrate observed using nitrate sensors mounted on profiling floats and to assess the utility of the annual nitrate drawdown as an estimator of ANCP in the Southern Ocean. Nitrate has the advantage, relative to oxygen and dissolved inorganic carbon, that no air-sea gas exchange is involved in the estimation of ANCP. As a result, absolute accuracy for the nitrate measurement is not required, although long-term consistency is a condition. Nitrate sensors have been deployed for years on profiling floats [*Johnson et al*., 2010, 2013; *Johnson and Claustre*, 2016; *Plant et al*., 2016; *Pasqueron de Fommervault et al*., 2015]. The protocols needed to correct data for long-term stability are well understood [*Johnson et al*., 2013, 2017]. As a result, long-term studies of ANCP, derived from the observations of annual nitrate drawdown, are possible [*Plant et al*., 2016]. Here we examine the nitrate data from 31 profiling floats that were deployed in the Southern Ocean and which have operated for at least 1 year.

2. Materials and Methods

2.1. Profiling Floats and Sensors

The data reported in this paper were collected using ultraviolet (UV) spectrophotometer nitrate sensors that have been deployed on profiling floats [*Johnson et al*., 2013]. Both in situ ultraviolet spectrophotometer (ISUS) sensors [*Johnson and Coletti*, 2002] and submersible ultraviolet nitrate analyzer (SUNA) sensors [*MacIntyre et al*., 2009] have been deployed. Data from 24 floats, from a total of 31 that operated from near 30°S to 69°S, are considered (Table 1). Of the seven floats not considered here, the nitrate sensors on five floats deployed near the Ross Sea fouled rapidly after deployment. This failure may have occurred due to the prevalence of *Phaeocystis antarctica* in the region. *Phaeocystis* sp. is known to produce gelatinous

Table 1. Winter Maximum and Summer Minimum Nitrate and ANCP Estimated From the Vertically Integrated Change in Nitrate[a]

		Date		LON	LAT	LON	LAT	950 m Salinity		Surf NO_3		NO_3 ANCP		POC ANCP	
WMO #	UW #	Max	Min	Max		Min		Max	Min	Max	Min	All	QC	All	QC
5904475	0037	Sep 2015	Dec 2015	10.2	−31.2	6.5	−27.8	34.34	34.39	2.5	1.0	0.0	0.0	−0.13	−0.13
5904476	0508	Sep 2015	Dec 2015	26.3	−46.3	30.4	−48.9	34.44	34.44	26.6	25.3	1.5	1.5	0.26	0.26
5901492	5146	Oct 2008	Jan 2009	52.2	−52.1	57.4	−52.6	34.68	34.69	28.2	28.2	−1.3	−1.3		
		Sep 2009	Jan 2010	69.0	−52.6	67.1	−50.4	34.63	34.65	29.4	27.1	1.4	1.4		
5902112	5426	Oct 2009	Jan 2010	294.2	−56.8	309.8	−52.8	34.39	34.44	26.3	22.5	1.5			
		Sep 2010	Mar 2011	322.7	−45.6	316.5	−44.7	34.44	34.36	23.0	4.4	13.8			
		Sep 2011	Jan 2012	318.5	−44.5	312.4	−42.9	34.38	34.34	15.1	3.6	3.4	3.4		
5903612	6967	Sep 2012	Dec 2012	9.2	−39.4	13.0	−41.7	34.32	34.28	5.6	−1.2	5.0	5.0		
		Sep 2013	Dec 2013	19.1	−42.6	21.0	−41.8	34.34	34.41	8.3	0.5	3.6			
5903718	6968	Sep 2012	Mar 2013	197.6	−50.0	210.0	−50.2	34.34	34.29	19.4	14.6	3.5		0.37	
		Sep 2013	Jan 2014	216.7	−51.6	234.0	−57.2	34.32	34.50	20.2	23.1	−5.6		0.91	
		Sep 2014	Mar 2015	254.8	−61.5	265.2	−63.9	34.63	34.65	31.2	28.2	2.2		0.50	
5903593	7552	Oct 2012	Mar 2013	97.0	−42.5	99.8	−44.5	34.40	34.41	9.8	6.1	2.7	2.7	0.31	0.31
		Oct 2013	Jan 2014	107.8	−42.9	107.2	−42.9	34.38	34.38	11.6	8.4	1.1	1.1	0.37	0.37
		Sep 2014	Mar 2015	108.4	−46.0	112.1	−45.1	34.40	34.36	13.4	9.5	3.1	3.1	0.33	0.33
		Oct 2015	Dec 2015	144.0	−51.3	154.1	−52.3	34.35	34.37	17.2	19.4	−2.7		0.46	
5903755	7553	Oct 2013	Feb 2014	258.5	−28.2	256.9	−29.1	34.36	34.33	0.6	0.8	0.1	0.1		
		Sep 2014	Mar 2015	258.0	−29.3	258.8	−29.5	34.32	34.31	0.5	0.3	0.4	0.4		
		Sep 2015	Jan 2016	261.1	−29.7	262.4	−28.8	34.32	34.35	0.6	0.7	0.1	0.1		
5904180	7613	Oct 2014	Feb 2015	202.6	−66.0	201.7	−65.8	34.72	34.72	31.9	28.2	2.0	2.0	0.24	0.24
		Oct 2015	Feb 2016	203.2	−65.4	204.9	−65.4	34.72	34.72	30.8	26.9	2.2	2.2	0.47	0.47
5904105	7619	Oct 2013	Feb 2014	146.5	−64.6	150.6	−65.0	34.70	34.72	35.8	30.6	1.9	1.9	0.15	0.15
5904104	7620	Oct 2013	Mar 2014	153.5	−64.2	154.5	−63.2	34.73	34.73	32.6	28.6	0.6	0.6	0.89	0.89
		Sep 2014	Mar 2015	151.5	−61.0	156.2	−60.0	34.73	34.74	34.3	27.4	3.4	3.4	0.81	0.81
5904467	7652	Oct 2015	Jan 2016	4.3	−60.8	4.9	−61.3	34.68	34.68	30.4	25.3	0.6	0.6	0.76	0.76
5904470	8514	Sep 2015	Feb 2016	143.7	−46.2	141.1	−45.6	34.39	34.39	12.3	5.8	2.5	2.5	0.34	0.34
5904396	9031	Sep 2014	Jan 2015	228.5	−52.6	230.6	−52.6	34.29	34.29	21.8	14.9	6.0	6.0	0.32	0.32
		Oct 2015	Jan 2016	240.4	−51.6	241.5	−48.9	34.32	34.29	19.7	13.7	3.5	3.5	0.35	0.35
5904185	9092	Sep 2015	Jan 2016	244.5	−60.9	252.5	−60.3	34.62	34.61	29.8	23.3	3.9		1.31	
5904471	9094	Oct 2015	Feb 2016	1.9	−66.1	2.6	−65.7	34.69	34.69	32.7	24.3	3.5	3.5	0.54	0.54
5904188	9095	Sep 2014	Feb 2015	219.5	−50.0	221.4	−50.6	34.31	34.30	16.2	10.3	4.2	4.2	0.27	0.27
		Oct 2015	Jan 2016	230.6	−53.9	233.2	−54.5	34.30	34.30	18.6	16.7	0.3	0.3	0.27	0.27
5904469	9096	Sep 2015	Mar 2016	359.6	−54.0	1.1	−54.3	34.71	34.71	31.3	26.5	2.1	2.1	0.53	0.53
5904468	9099	Oct 2015	Feb 2016	2.2	−64.6	4.2	−64.2	34.68	34.68	33.1	24.9	2.7	2.7	0.72	0.72
5904397	9125	Oct 2015	Feb 2016	358.4	−62.0	354.6	−61.2	34.67	34.67	31.8	27.3	1.2	1.2	0.52	0.52
5904395	9254	Oct 2014	Feb 2015	211.5	−40.0	209.6	−39.1	34.31	34.31	3.9	2.8	0.5	0.5	0.16	0.16
		Sep 2015	Jan 2016	205.6	−39.0	206.8	−39.3	34.31	34.32	4.8	2.8	−0.2	−0.2	0.12	0.12
5904473	9260	Oct 2015	Mar 2016	45.2	−47.9	47.5	−42.6	34.54	34.51	27.0	19.7	4.1	4.1	0.58	0.58
5904472	9275	Oct 2015	Feb 2016	347.3	−68.4	343.4	−68.6	34.69	34.69	30.2	25.5	1.4	1.4	0.56	0.56
5904474	9313	Sep 2015	Mar 2016	12.7	−42.7	12.9	−40.2	34.30	34.32	14.7	3.0	10.8		0.26	

[a]ANCP values estimates from the accumulation of POC are also shown. ANCP columns labeled QC show only values that pass the criteria outlined in the text. ANCP units are mol C m^{-2} yr^{-1}. WMO # is the World Meteorological Organization designation for the float and UW # is the University of Washington serial number.

aggregates that may foul optics [*MacKenzie et al*., 2002]. This problem appears to have been largely eliminated by removing the ISUS sensor optics from the flow stream of the CTD [*Johnson et al*., 2017]. Exposing the optics to the surface ocean has allowed waves to clean the optics when floats surfaced. Fouling of nitrate sensors has been much less frequent after instruments received this modification. The nitrate sensor failed electronically on another float and the sensor failed on one additional float shortly after deployment for unknown reasons.

Sixteen of these floats with useful data were deployed as part of the Southern Ocean Carbon and Climate Observations and Modeling (SOCCOM) program and eight were deployed prior to SOCCOM. The floats generally profiled every 5 or 10 days from a maximum depth that ranged between 1000 and 2000 m [*Johnson et al*., 2017]. In addition to nitrate sensors, the floats also carried Aanderaa oxygen optodes, WET Labs FLBB or MCOMS bio-optical sensors that measure backscatter, and Deep-Sea DuraFET pH sensors.

Nitrate concentration was calculated according to Argo protocols [*Johnson et al*., 2016]. Processing included a pressure coefficient of −2.6%/1000 dbar for the absorptivity of sea salt. The presence of this effect was suggested by *Pasqueron de Fommervault et al*. [2015]. It was subsequently confirmed by laboratory measurements at MBARI. The pressure coefficient was implemented in the calculation of nitrate as described by *Johnson et al*. [2016, equation 7].

3. Data Sources and Quality Control Procedures

All data used in this paper were downloaded from the SOCCOMViz web site. Only quality controlled data obtained at ftp://ftp.mbari.org/pub/SOCCOM/FloatVizData/QC/ were used. In addition, all of the data are made available through the Argo Global Data Assembly Centers, which will serve as the final archive. Note that at the SOCCOM data archive float data files are currently identified by their University of Washington serial number (Table 1). At the Argo GDAC, floats are identified by their World Meteorological Organization (WMO) number (Table 1). The SOCCOM data system is currently converting to utilize only WMO numbers, but at the time this paper is being written, both designations are in use.

3.1. QC and Adjustment Procedure

Once a profiling float is deployed, the nitrate measurements often have to be adjusted to correct for offsets and temporal drifts in the measurement that impact accuracy. These shifts in accuracy can occur from fouling of the optical path over time, or due to subtle changes in the optics and electronics that result from handling prior to deployment and in situ changes such as the penetration of water into the optics. Fortunately, such changes are independent of concentration, pressure, or temperature, so only a single adjustment is needed to correct the concentrations at all depths on each profile [*Johnson et al*., 2013, 2017].

The procedures used to adjust nitrate data are discussed in detail elsewhere [*Johnson et al*., 2017] and are only briefly summarized here. Corrections for offsets in sensor accuracy at deployment and changes over time are achieved by comparing data at depth (1000 or 1500 m depending on the maximum profile depth), where the nitrate concentration is most stable, to multiple linear regression (MLR) estimations of nitrate concentration at the same depth. The MLR equations are derived from laboratory measurements on water samples collected throughout the Southern Ocean [*Williams et al*., 2015, 2016]. The adjustments are verified by comparing the corrected data estimates generated from a neural network-based procedure [*Sauzède et al*., 2017] and data from GLODAPv2 [*Olsen et al*., 2016]. The adjustment process produces a data set that matches samples collected at stations where floats are deployed to better than 1 μmol kg^{-1} throughout the water column [*Johnson et al*., 2017]. The same methods are used to correct for sensor errors as the float moves through the Southern Ocean and there should be no additional degradation in sensor accuracy with time [*Johnson et al*., 2017].

4. Results and Discussion

A map of the profiling float launch positions and their trajectories is shown in Figure 1. These floats have all operated through at least one full year with nitrate data that passes our quality control checks. These data now enable a synoptic, three-dimensional view of the spatial and time varying concentration of nitrate in the Southern Ocean (Figure 2). The annual cycles in nitrate concentration, due to the seasonal variations in phytoplankton uptake of nitrate, remineralization of organic matter and upward transport by ocean physics are clearly visible in the float data, as is the general decrease in surface nitrate concentration found toward the equator (Figure 3). Exceptions to a smooth annual cycle occur when floats cross the major Southern Ocean frontal boundaries that separate distinctly different water masses. For example, float 5904396/9031 (WMO number/UW number; Table 1) drifted north from Subantarctic waters into subtropical waters and temperature increased while nitrate concentrations dropped significantly (Figure 3).

In addition to nitrate, nearly all of our profiling floats carry bio-optical sensors for backscatter at 700 nm. The signal from the backscatter sensors was processed to yield backscatter due to particles (b_{bp}) by subtracting the scattering signal due to water [*Schmechtig et al*., 2016]. The concentration of suspended particulate organic carbon (POC) was then estimated from the b_{bp} values. A linear relationship between the concentration of POC measured in samples at the time floats were launched and the b_{bp} values measured on the first float profile has been reported [*Johnson et al*., 2017]:

$$\mathrm{POC}\ [\mathrm{mmol\ m^{-3}}] = \left(3.12\times10^{4}\times b_{bp}+3.04\right)/12 \quad (1)$$

The relationship in equation (1) is very similar to that reported by *Cetiníc et al*. [2012] in the North Atlantic, which suggests little geographic bias. The RMS error of the observed data about the line in equation (2) was 35 mg m^{-3} (3 mmol m^{-3}) [*Johnson et al*., 2017]. Estimated POC concentrations are likely accurate to within this scatter. Time series of POC concentration in the upper 30 m are shown in Figure 3. POC concentration

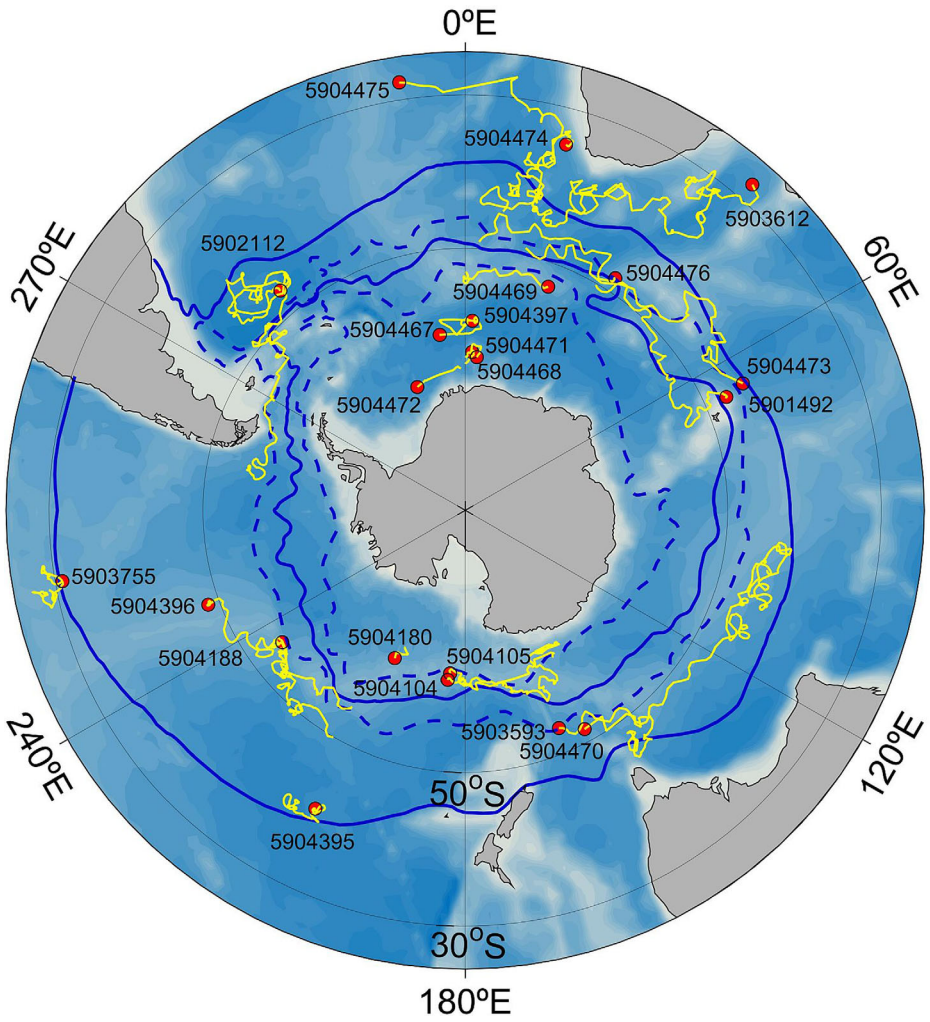

Figure 1. Map of Southern Ocean biogeochemical profiling floats for which NCP estimates were derived. Floats are identified by their WMO number. Latest float positions (red circles), float tracks (yellow). Oceanographic boundaries [*Orsi et al.*, 1995] are in blue and listed by decreasing distance to Antarctica. Subtropical Front (solid blue), Subantarctic Front (dashed blue), Polar Front (solid blue), and Southern Antarctic Circumpolar Current Front (dashed blue).

clearly increases each summer as nitrate was drawn down, reaching maximum values near the time of the minimum in nitrate.

4.1. Annual Nitrate Drawdown

The annual nitrate drawdown, due to biological uptake of nitrate, was determined from the change in the vertically integrated stock of nitrate observed by each profiling float. The annual cycles of surface nitrate, including those shown in Figure 3, were analyzed to find the late winter maximum concentration and spring to summer minimum concentration. Vertical profiles of nitrate, temperature, and salinity at the times of the maximum and minimum nitrate concentrations are shown for several floats in Figure 4. The summer depletion in nitrate is clearly seen for floats south of the subtropics and the depletion extends to depths as great as 200 m (float 5904188/9095, Figure 4).

We estimated the annual drawdown of nitrate as the vertical integral to 200 m of the decrease in nitrate (winter-summer concentration), as shown in Figure 4. For each float, the profile with the highest nitrate in the months of August through November was found. The mean nitrate profile for that month was then computed and used as the austral winter maximum. Similarly, the profile with the lowest nitrate concentrations during December through March was found and the austral summer profile minimum was computed as the mean for the month in which that profile fell. Monthly average nitrate profiles were used to minimize

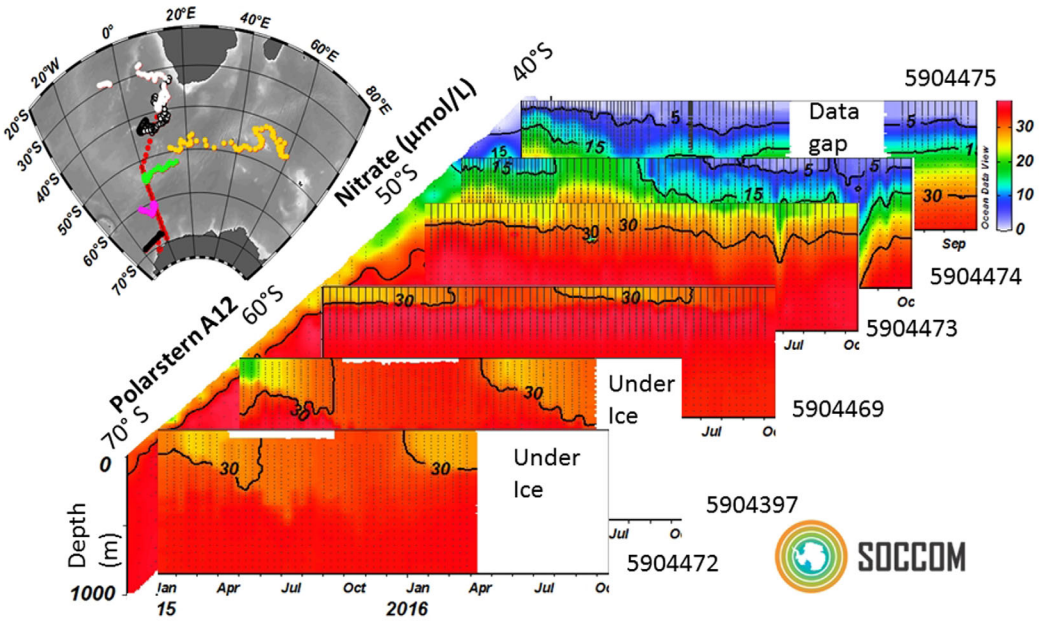

Figure 2. Nitrate concentration in the upper 1000 m determined on the Polarstern along the GO-SHIP A12 line in December 2014 to February 2015 shown on the diagonal along with time/depth sections of nitrate concentration determined by profiling floats deployed by the Polarstern. Gaps in the data for floats 5904472 and 5904397 occur while the floats were under ice. The missing data have since been returned, but not in time for this analysis. A data gap for 5904475 occurred due to a malfunction in the buoyancy engine of the float. Inset map shows the float trajectories.

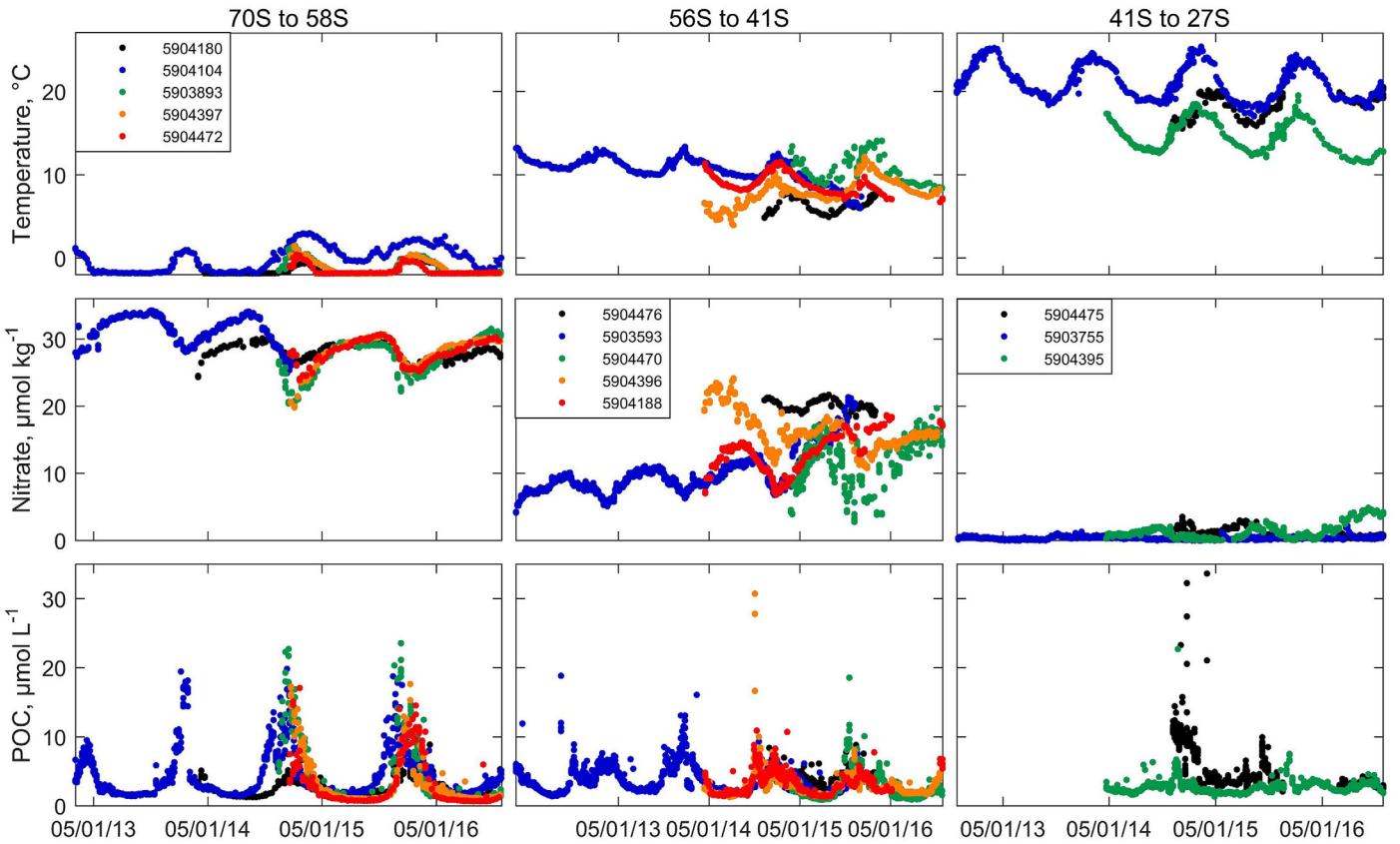

Figure 3. (top) Temperature, (middle) nitrate, and (bottom) POC concentrations versus time in the upper 30 m of the water column for 13 of the floats analyzed here. Floats are grouped by latitude. (left) Floats in the seasonal ice zone (69°S–58°S), (middle) the subpolar region (56°S–41°S), and (right) The subtropical zone (41°S–27°S).

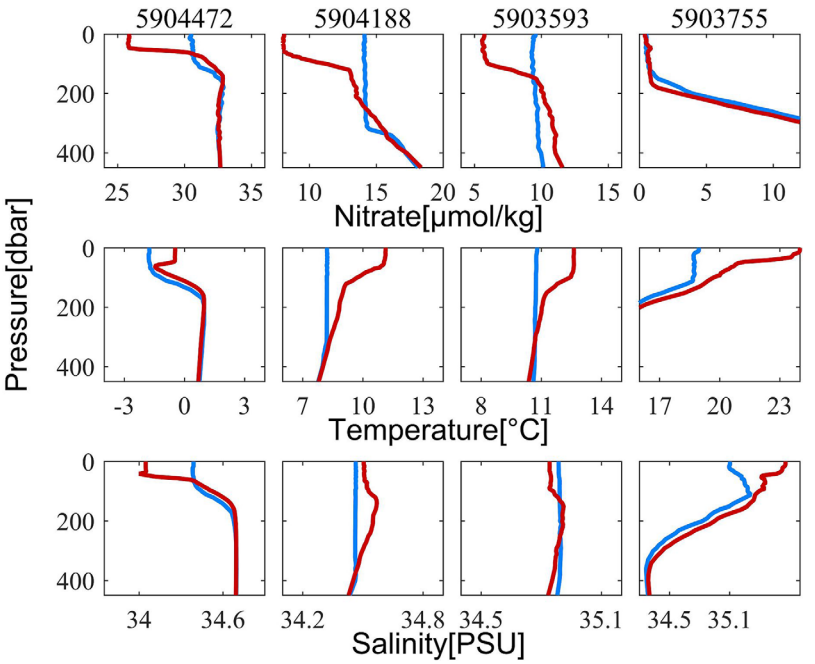

Figure 4. Winter (blue) and summer (red) nitrate, temperature, and salinity profiles for floats 5904472 (seasonal ice zone), 5904188 and 5903593 (subpolar zone), and 5903755 (subtropical zone). Profiles are the monthly average (typically three float profiles) of the months with highest and lowest nitrate in the upper 30 m.

the impact of short-term oscillations in mixed layer depth due to internal waves. The integrated, annual nitrate drawdown was then converted to carbon units using a Redfield ratio of 106 C:16 NO_3^-. This value was used as the estimate of ANCP at each location. The estimated ANCP values are summarized in Table 1.

At depths below 200 m, there is generally good agreement between the summer and winter nitrate profiles (Figure 4). Exceptions to this occur when there are large changes in salinity at depth. These salinity changes indicate that the float has moved from one water mass to another, perhaps by crossing a front. The nitrate concentration shifts from winter to summer for such floats are corrupted by the water mass change in these cases and they were excluded from analysis as discussed below.

Surface salinity changes that occur from winter to summer (Figure 4c) have a less clear indication of interference on the interpretation of the seasonal nitrate concentration change. At high latitudes, low salinity in summer results from ice melt (float 5904472, Figure 4c). This dilution has little impact on the calculated value of the annual nitrate concentration change. In the subtropics (float 5903755, Figure 4c), the seasonal salinity change is driven, to a large extent, by excess evaporation over precipitation in summer and again has little impact on nitrate concentration.

The potential interference from surface salinity changes in the Subantarctic and Polar Frontal Zones is less clear. *Lourey and Trull* [2001] examined nitrate and salinity changes along repeat hydrography lines south of Tasmania. They argue that salinity changes there occur due to seasonal shifts in the position of the frontal system and the shift in water masses is partially responsible for the seasonal nitrate concentration change. As a result, they use a well-defined relationship between salinity and nitrate, which is replicated in our results, to correct the observed annual nitrate drawdown for this effect before estimating ANCP. *Lourey and Trull* [2001] used this relationship when examining data in a fixed, Cartesian coordinate system. Such a treatment may not be appropriate for an array of floats for two reasons. Profiling float data sets more closely approximate a Lagrangian framework as the floats drift at depth. Second, our array of floats is widely distributed on a global scale. It is unlikely that seasonal migration of Southern Ocean frontal systems are a widespread occurrence given that frontal positions are linked to deep topography with little seasonal variability in most regions [*Moore et al*., 1999].

To assess the potential effect of upper ocean salinity changes on ANCP computed from the seasonal nitrate drawdown, we tried correcting the nitrate data for salinity changes as indicated by *Lourey and Trull* [2001].

This produced a change in the mean ANCP for the entire data set less than 10%. However, it produced large changes in the estimated ANCP in the seasonal ice zone and subtropics that are of opposite sign, as shown by the salinity profiles in Figure 4. These differences occur because the salinity changes there are driven by processes other than the water mass movements that the *Lourey and Trull* [2001] method is designed to correct. Those ANCP values corrected by the *Lourey and Trull* [2001] method in the seasonal ice zone and subtropics are not correct. In the subpolar regions that include the Subantarctic and Polar Frontal Zones, there are changes both positive and negative in salinity and in the ANCP values corrected with the *Lourey and Trull* [2001] method, as expected from the salinity profiles shown in Figure 4. The net effect is small for zonal means. Because of the confounding factors of salinity changes to the south and north, surface salinity changes were not used to correct nitrate concentration.

We chose to integrate to a constant depth, rather than to the mixed layer depth, for reasons outlined by *Stephenson et al.* [2012] in their assessment of upper ocean heat content in the Southern Ocean. The integration to 200 m exceeds the maximum depth at which there were measureable differences in the winter and summer nitrate profiles in all but a few cases (float 5904188/9095, Figure 4). The integration could have been carried to greater depths or to a depth where the summer nitrate profile diverges from the winter profile, but these alternatives do not produce a marked change in the results. As one of our goals was to find simple, automated methods to estimate ANCP, which can be derived from the annual nitrate drawdown, we have selected a constant integration depth of 200 m. Further, by extending the integration to 200 m, below the nitracline, we minimize the seasonal change in integrated nitrate stocks associated with vertical diffusion across a steep gradient.

In the subtropics, where nitrate concentrations were near zero and below sensor detection limits, no significant change in nitrate concentration profile was observed from winter to summer other than a slight deepening of the nitracline in summer (float 5903755/7553, Figure 4). This change in the nitracline, seen previously near Hawaii [*Letelier et al*., 2004], may reflect a deepening of the compensation depth during longer summer days. This allows phytoplankton to access nitrate at greater depths than in winter. In our calculations, it was the only contribution of nitrate to the ANCP calculation in oligotrophic waters.

Our estimates of annual nitrate depletion neglect any inputs into the upper 200 m by vertical advection (upwelling) or by horizontal transport of nitrate and ascribe all of the nitrate change to biological processes. Previous estimates of ANCP have generally incorporated estimates of physical transport, which are derived from a variety of methods, into the mass balance. For example, the estimate of ANCP from the annual drawdown in nitrate made by *MacCready and Quay* [2001] included mass balance contributions from vertical transport and Ekman transport to the observed nitrate concentration change. The advective terms are, in most cases, considerably smaller than the ANCP term in the *MacCready and Quay* [2001] budgets. A more recent analysis in the Drake Passage area [*Munro et al*., 2015] yields similar results. However, studies with one-dimensional models have found that reproducing the observed property distributions requires additional inputs, which may represent horizontal advective terms [*Wang et al*., 2003]. Further, eddy transport of biogeochemical tracers along meridional gradients can counteract the estimated horizontal transport along mean gradients [*Ito et al*., 2010].

A complete analysis of the influences of ocean physics on the nitrate mass balance is likely to require a high resolution model to assess the influence of advective terms on the mass balances. Such a detailed analysis is beyond the scope of this work. However, we have performed a preliminary assessment of the influence of vertical and meridional transport by comparing the vertically integrated, annual nitrate drawdown with the particulate carbon export from 100 m depth (Export Production) in the ESM2M coupled Earth System Model [*Dunne et al*., 2013]. In regions with persistent surface nitrate throughout the year, we find that ANCP and Export Production are roughly equal at a steady state and with suitable spatial averaging, as expected [*Falkowski et al*., 2003]. Zonal means of the integral of the seasonal nitrate drawdown in the upper 100 m, after conversion to carbon units, and the particulate carbon export below 100 m in the ESM2M model are shown in Figure 5 along with the ratio of these quantities. If the nitrate concentration change is heavily biased by ocean physics, then these quantities will not agree. The ratio of these quantities is generally within 20% of 1. The near balance of ANCP from the modeled nitrate drawdown without a correction for physical transport and the modeled Export Production indicates that ocean physics produces a bias less than 20% in the zonal mean south of 35°S. This analysis was done at fixed, Cartesian coordinates and it is possible that the bias from float observations is even smaller than 20% due to the Lagrangian nature of the

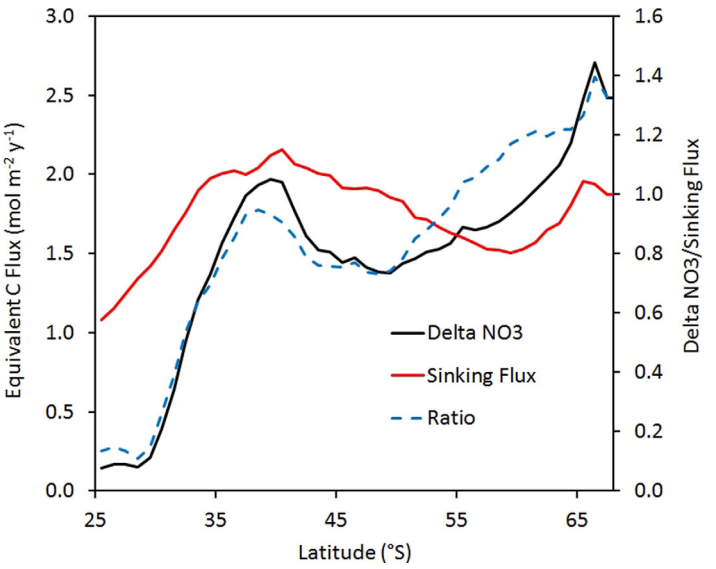

Figure 5. The carbon flux computed from the integrated annual nitrate drawdown determined in the ESM2M model, after conversion to C units by the Redfield ratio (black), and the annually integrated sinking flux of carbon at 100 m (red). The ratio is shown as a blue dashed line.

float data. The exception to this conclusion occurs in subtropical waters at latitudes lower than 35°S, where the ratio drops to near zero. The disagreement in subtropical waters represents the well-known conundrum of high ANCP in the presence of little or no dissolved nitrate [*Johnson et al.*, 2010]. ANCP from the nitrate drawdown in subtropical waters should underestimate the correct ANCP value and Export Production.

The agreement between model derived annual nitrate drawdown and sinking carbon fluxes at latitudes south of 35°S (Figure 5) supports our presumption that the nitrate drawdown is dominated by biological processes and the bias due to ocean physics is relatively small (~20% or less). These conclusions will, of course, only apply when looking at a reasonably large number of floats that are distributed throughout the Southern Ocean, as local exceptions can certainly occur. Errors in the annual nitrate drawdown calculation will occur if a float moves between water masses with distinctly different nitrate concentrations in the upper 200 m. This is particularly true for floats that have a large change in latitude, as meridional nitrate gradients are large. To control for this possibility, we have filtered out data (Table 1) based on the following criteria. If the salinity below 500 m changed by more than 0.05 from winter to summer, if the float moved more than 8° in longitude or 5.5° in latitude, then the estimates of ANCP were not used in subsequent calculations.

The ANCP values that were derived from the annual nitrate drawdown would be overestimates, relative to the amount of carbon exported by the biological pump, if large amounts of organic nitrogen remained in the upper ocean after the summer minimum in nitrate concentration and this organic nitrogen was then subsequently returned to the nitrate pool by remineralization of the organic matter. The POC time series (Figure 3) show that POC clearly accumulated in the upper water column during summer. However, if we assume that the POC had a C/N ratio similar to the Redfield ratio, then the POC concentrations shown in Figure 3 cannot supply enough organic nitrogen to bias the estimated value of ANCP by more than 20%, except in the most oligotrophic waters. For example, we can estimate the ANCP from the production of POC detected in the upper 200 m by the backscatter sensors. We take ANCP based on POC as the difference in the winter minimum in the vertical integral of POC to 200 m and the summer maximum using monthly averages as for the nitrate estimate. The ANCP

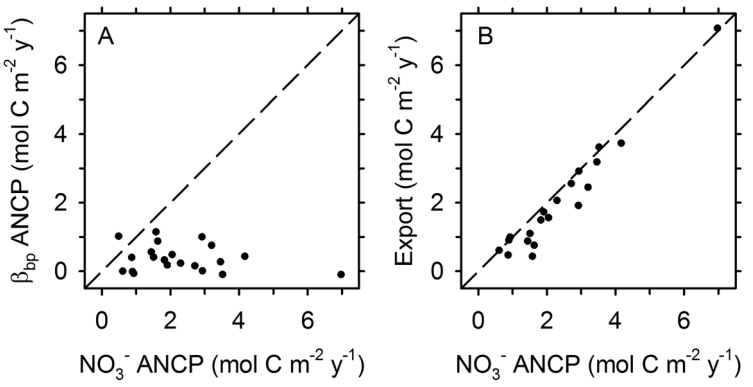

Figure 6. (a) Annual net community production estimated from the buildup of biomass recorded by the backscatter sensor on each float versus the ANCP estimated from the annual drawdown of nitrate. Dashed line is the 1:1 relationship. (b) ANCP that has been exported, computed as ANCP from annual nitrate drawdown minus ANCP from biomass, versus ANCP from annual nitrate drawdown.

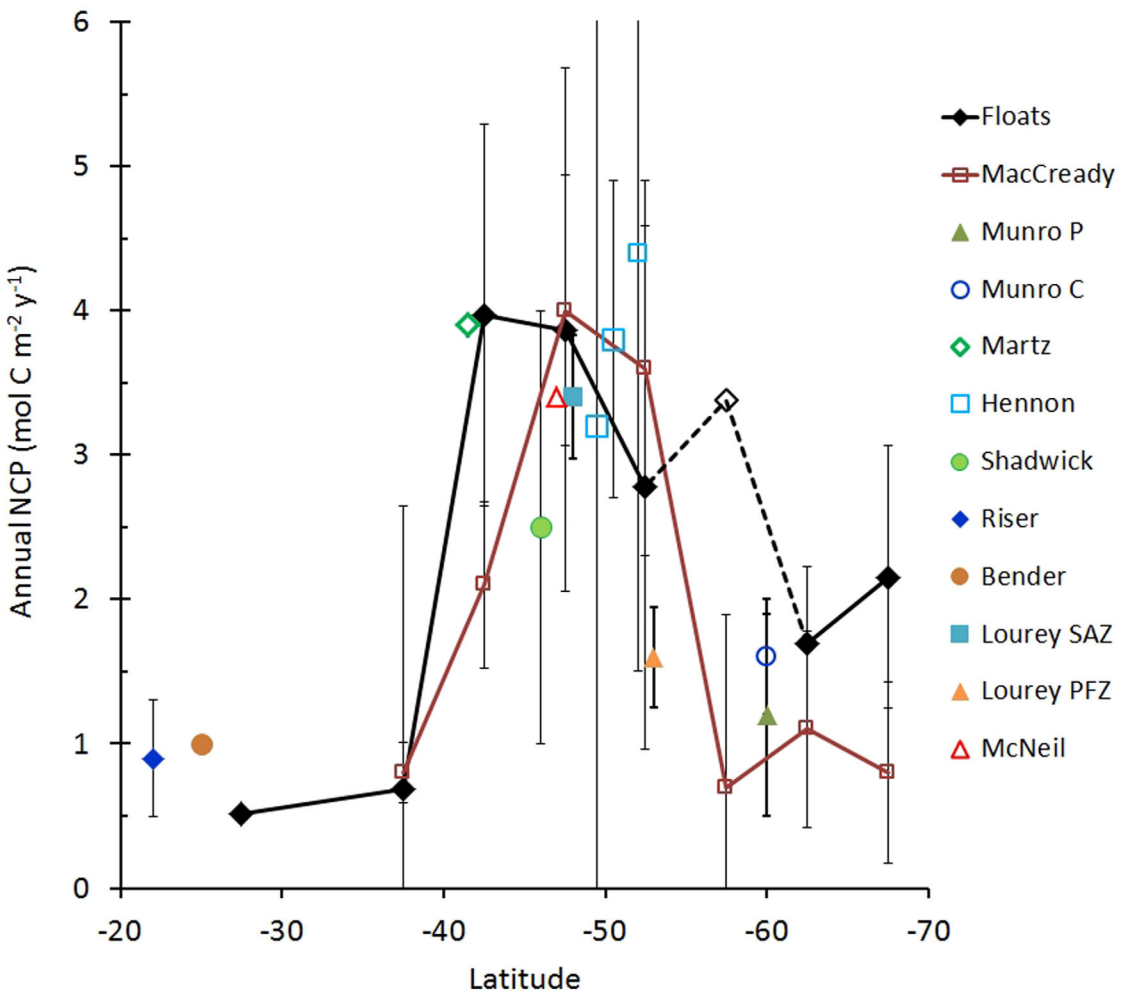

Figure 7. ANCP estimated from annual nitrate drawdown observed by floats and binned by 5° latitude bands. Error bars at 90% confidence intervals based on the standard deviation of all data in each band. There is only one value in the 55°–60° band and it is connected by a dashed line. Results of *MacCready and Quay* [2001], *Munro et al*. [2015] using P or C observations, *Martz et al*. [2008], *Hennon et al*. [2016], *Lourey and Trull* [2001], *McNeil and Tilbrook* [2009], *Shadwick et al*. [2015], *Riser and Johnson* [2008], and *Bender and Jönsson* [2016] are shown for comparison.

values derived in this manner are substantially lower than those derived from the annual drawdown of nitrate. The POC-based estimates of ANCP seldom exceeded 1 mol C m^{-2} yr^{-1} (Figure 6a). The mean ANCP derived from POC was 0.4 mol C m^{-2} yr^{-1}, compared to a mean of 1.9 mol C m^{-2} yr^{-1} for values derived from nitrate in the subset of floats with bio-optical sensors (Table 1). The fivefold difference cannot be accounted for by the expected error in POC concentrations that was estimated above.

These results indicate that the nitrate lost from the water column during summer does not substantially accumulate in the particulate pool. It is also unlikely that there is substantial seasonal build up in the dissolved organic nitrogen pool. In the few cases where the DON or DOC contributions to Export Production have been estimated in the literature [*Lipschultz*, 2001; *Knapp et al*., 2005; *Hansell and Carlson*, 2001], it has been less than the contribution from particulate matter. Therefore, we do not expect that the ANCP estimates would be substantially biased by dissolved organics. Most of the missing nitrate must have been exported with little delay after it was produced (Figure 6b).

The ANCP estimates derived from the annual nitrate drawdown were binned by 5° bands in latitude and the resulting mean values are plotted in Figure 7. Error bars for each latitude band were computed as the 90% confidence interval using the standard deviation of all ANCP estimates in that band. These error bands are large and there is not a significant difference between different latitude bands, given the number of annual cycles used in the computations. However, the trends appear fairly robust, as they are consistent

Table 2. Estimates of Southern Ocean NPP (Pg C yr^{-1}) for the Ocean Area South of 50° South[a]

Arrigo et al. [1998]	4.4
Moore and Abbott [2000]	2.8
Arrigo et al. [2008]	1.9
Shang et al. [2010] VGPM	1.3
Shang et al. [2010] CbPM	1.7
Leung et al. [2015] 16 CMIP5 models	5.0 ± 2.5 (1.0–9.7)
Float ANCP/*ef* ratio (0.35)	3.7

[a]The mean and standard deviation for the CMIP5 model suite is given, with the range of results shown in parentheses. Estimates from *Shang et al.* [2010] were generated by multiplying their mean rates by the appropriate Southern Ocean area.

with a variety of other observations discussed below, as well as the trends in the ESM2M model shown in Figure 5. As the number of floats and years of data increase, these error bands will likely decrease rapidly.

Southern Ocean ANCP values reported by *MacCready and Quay* [2001] are shown for comparison (Figure 7). MacCready and Quay considered the potential contribution of remineralization of organic matter in the mixed layer on their ANCP estimate. They also felt that a strong remineralization effect was unlikely. We have utilized their results which explicitly neglect possible remineralization effects [*MacCready and Quay*, 2001, Table 2]. Both our results and those of *MacCready and Quay* [2001] show maximum values for the integrated ANCP between 40°S and 50°S that are near 4 mol C m^{-2} yr^{-1}. The maximum in the profiling float estimate is shifted a bit further north, but given the uncertainty in the ANCP estimates, the differences are likely not significant.

As both our computations and those of *MacCready and Quay* [2001] have similar underlying assumptions, we have also considered a variety of other, independent assessments of ANCP to verify our results. These comparisons are also shown (Figure 7). *Munro et al.* [2015] have reported ANCP values using 9 years of data for the phosphate and the DIC concentration (computed from measurements of pCO_2) that were observed at near monthly intervals in the Drake Passage. Their results are 1.2–1.6 mol C m^{-2} yr^{-1}. *Martz et al.* [2008] reported the annual carbon export in the Pacific sector of the Southern Ocean using oxygen sensors on an array of profiling floats deployed between New Zealand and Chile to determine the integrated respiration rate in the mesopelagic zone. They found a carbon export of 3.9 mol C m^{-2} yr^{-1}. *Hennon et al.* [2016] extended this work to the Indian and broad regions of the Pacific sectors of the Southern Ocean. They found annual carbon export rates of 3.8 ± 1.1 and 3.2 ± 3.2 mol C m^{-2} yr^{-1} in each location. *Hennon et al.* [2016] also report one additional value, which they labeled Drake Passage. This set of floats has a mean value of 4.4 ± 2.9 mol C m^{-2} yr^{-1}, which appears at odds with the *Munro et al.* [2015] result. However, the floats in this array have only passed through the Drake Passage and most of the data comes from the Argentine Basin, an area of high NCP [*Schlitzer*, 2000; *Dunne et al.*, 2007]. That data point is plotted in Figure 7 at a latitude near the Argentine Basin and not the Drake Passage. *Lourey and Trull* [2001] and *McNeil and Tilbrook* [2009] report ANCP values from repeat occupations of hydrographic lines south of Tasmania. *Lourey and Trull* [2001] use annual changes in nitrate to obtain values of 3.4 mol C m^{-2} yr^{-1} in the Subantarctic Zone and 1.6 mol C m^{-2} yr^{-1} in the Polar Frontal Zone. *McNeil and Tilbrook* [2009] obtain a value of 3.4 mol C m^{-2} yr^{-1} using DIC. *Shadwick et al.* [2015] report an ANCP value of 2.5 ± 1.5 mol C m^{-2} yr^{-1} using pCO_2 sensors on the SOTS mooring south of Tasmania. *Bender and Jönsson* [2016] reported ANCP values near 1 mol C m^{-2} yr^{-1} based on DIC distributions measured on hydrographic lines between 20°S and 30°S and 140°W and 110°W in the Pacific. *Riser and Johnson* [2008] reported an ANCP value of 0.9 ± 0.4 mol C m^{-2} yr^{-1} using dissolved oxygen observed by a single profiling float near 20°S and 120°W in the South Pacific. These values are all generally consistent with the profiling float nitrate measurements (Figure 7). They outline a similar meridional distribution of ANCP, with lower values at highest latitudes and in the subtropics, and a maximum near 40 to 50°S.

The area weighted value of ANCP for all stations is 2 and 2.9 mol C m^{-2} yr^{-1} for all regions south of 40°S. These values fall within the range of ANCP values summarized by *Emerson* [2014] of 3 ± 1 mol C m^{-2} yr^{-1}. However, most of the ANCP values reported by *Emerson* [2014] come from oligotrophic ocean areas with little or no nitrate in the surface waters. Our ANCP estimate for the region north of 40°S, where nitrate is generally near zero, is 0.56 mol C m^{-2} yr^{-1}, which is significantly less than the values in ESM2M (Figure 5) and the values that *Emerson* [2014] summarizes for the oligotrophic ocean. This difference is one of the classical conundrums of modern marine biogeochemistry. Large amounts of ANCP occur in the oligotrophic ocean when estimated using direct measurements of dissolved inorganic carbon or oxygen [*Gruber et al.*, 1998; *Keeling et al.*, 2004; *Johnson et al.*, 2010; *Emerson*, 2014]. However, there is never enough nitrate or phosphate present to support such high levels of ANCP [*Michaels et al.*, 1994; *Karl et al.*, 2003]. A seasonal

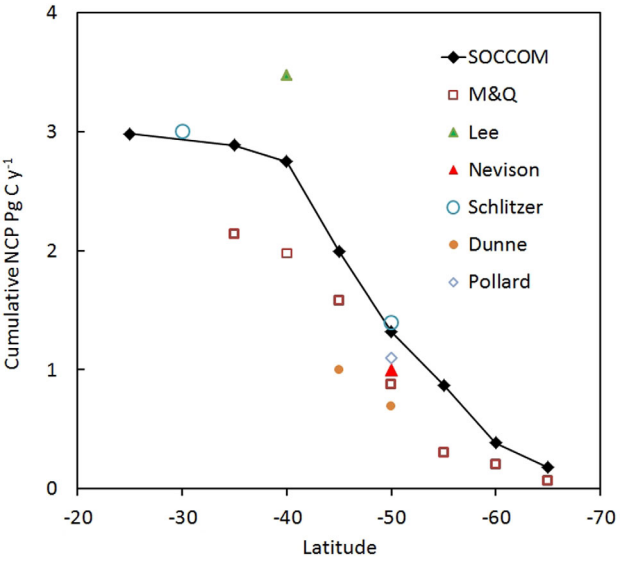

Figure 8. Cumulative ANCP values from Figure 7 integrated from South to North and plotted versus latitude. Results reported by *MacCready and Quay* [2001], *Lee* [2001], *Nevison et al*. [2012], *Schlitzer* [2002], *Dunne et al*. [2007], and *Pollard et al*. [2006].

drawdown in nitrate cannot match the ANCP values summarized by *Emerson* [2014] in oligotrophic regions. A variety of hypotheses have been advanced to address this discrepancy [*Johnson et al*., 2010]. While the issue remains under discussion, it is not surprising that our ANCP estimates made in oligotrophic waters are lower than carbon or oxygen-based values (Figure 7).

The cumulative ANCP, computed from south to north, was determined by multiplying the mean value of the integrated ANCP in each latitude band by the ocean area found in each band. The resulting distribution is shown in Figure 8. There are a variety of estimates of the cumulative ANCP in the Southern Ocean over various latitude spans and these are shown as well. The cumulative ANCP from south of 50°S, computed from the float data, is 1.3 Pg C yr^{-1}. Five independent estimates of cumulative ANCP or export flux to 50°S are available (Figure 8). These estimates are based on annual cycles in nitrate [*MacCready and Quay*, 2001], annual cycles in atmospheric potential oxygen [*Nevison et al*., 2012], inverse models of carbon and nutrient distributions [*Schlitzer*, 2002], an analysis of sinking carbon fluxes [*Dunne et al*., 2007], and upward flux of nitrate [*Pollard et al*., 2006]. They have a mean of 1.01 $\pm$ 0.3 (1 SD) Pg C yr^{-1}. The good agreement of all of these observations by a variety of methods, including observations in the ocean and in the atmosphere, is strong evidence that profiling floats with nitrate sensors can provide accurate measurements of ocean ANCP in high nutrient regions.

The cumulative ANCP south of 40°S, which spans the region of the Southern Ocean with excess nutrients at the surface, is 2.75 Pg C yr^{-1}. *Lee* [2001] reported a value of 3.5 Pg C yr^{-1} for this region, in reasonable agreement with the profiling float estimate. Global estimates of ANCP or carbon export, based on in situ observations, range from 8 Pg C yr^{-1} [*Lee*, 2001] to 9.6 Pg C yr^{-1} [*Dunne et al*., 2007] to 11 Pg C yr^{-1} [*Schlitzer*, 2000]. These values yield a mean for the global estimate of cumulative ANCP near 10 Pg C yr^{-1}. The nutrient rich Southern Ocean south of 40°S accounts for about 28% of the total ANCP or carbon export based on profiling float data. This region includes 23% of global ocean surface area, which suggests that the Southern Ocean ANCP is not disproportionately represented, given the uncertainties in the ANCP values. The cumulative ANCP from floats south of 50°S is 13% of the global ocean ANCP in about 14% of the ocean area, which again indicates no large bias per unit area. This stands in contrast to satellite-based estimates of primary production, which find only 5% of global primary production in this region of the Southern Ocean [*Carr et al*., 2006].

Satellite-based estimates of net primary production (NPP = primary production minus respiration by primary producers) are the current, observational metric for biologically driven carbon cycling in the global and Southern Ocean. Estimates of Southern Ocean NPP at latitudes south of 50°S derived from satellite remote sensing data and from an analysis of 16 biogeochemical models that were included in the CMIP5 Earth System Model suite are shown in Table 2. The earliest estimates of NPP based on remote sensing are about a factor of two higher than more recent NPP values, and all are less than the mean of the CMIP5 model suite. Assuming the equivalence of Export Production and net community production over annual cycles, we can relate ANCP and NPP through the *ef* ratio:

$$ef = \mathrm{ANCP}/\mathrm{NPP} \quad (2)$$

Estimates of the *ef* ratio in the Southern Ocean range from 0.18 to 0.58 [*Laws et al*., 2000, 2011] and they average 0.35. This is similar to the value (0.33) that was derived by *Nevison et al*. [2012] for the Southern

Ocean. The mean *ef* ratio was combined with the cumulative ANCP determined from float nitrate south of 50° to yield an estimated NPP for this region of 3.7 Pg C yr^{-1}. The mean of the CMIP5 model suite is reasonably close (35%) to the float-based estimate, although individual models may differ by 300%. Recent satellite-based estimates of NPP tend to be low of the float estimate by a factor of two, while the oldest satellite estimates are reasonably close to the values derived from the float data. Spatial bias in the float data could account for some of this difference. However, we note above that the float data are quite consistent with a variety of other ANCP estimates. Spatial bias is not likely a factor.

The mean and 90% confidence interval for all of the cumulative ANCP estimates at 50°S (Figure 8) is 1.0 ± 0.06 Pg C yr^{-1}. The recent satellite estimates of NPP are near 1.5 Pg C yr^{-1}, which implies an *ef* ratio of 0.67. The bulk of the evidence summarized by *Laws et al*. [2000, 2011] points to an *ef* ratio closer to 0.3. *Carr et al*. [2006] compared the performance of 24 algorithms used to predict NPP from satellite data at locations around the globe and found the greatest discrepancies between the algorithms in the Southern Ocean. This suggests relatively large uncertainty in Southern Ocean NPP derived from satellite ocean color observations and perhaps a systematic bias low by a factor of two.

5. Conclusions

The data reported in this paper have been generated after the deployment of 31 profiling floats with nitrate sensors. Eight floats were deployed between 2008 and 2013. Twenty-three of the floats were deployed in 2014 and 2015, with most of the 40 float years of data falling in 2014–2016. The results show clearly the potential to generate ANCP estimates that are consistent with previous measurements that have been made by a variety of methods. The number of floats that are capable of these measurements is growing rapidly. The SOCCOM program has deployed an additional 33 floats that have operated less than 1 year at the time this paper was written. An additional 40 floats will be deployed by the SOCCOM program during the current Austral summer. This will enable greater spatial resolution of NCP in the Southern Ocean and interannual estimates of variability in this process.

The zonally averaged distribution of ANCP estimates (Figure 7) shows a distinct pattern, with low values within the seasonal ice zone and low values in the subtropical zone at the northern limits of our data set. ANCP reaches a maximum in the latitude band between 40° and 50° S. This pattern is consistent with a variety of independent measurements using several techniques. In particular, the measurements of oxygen respiration rates in the mesopelagic zone with profiling floats [*Martz et al*., 2008; *Hennon et al*., 2016], which are measures of Export Production, match closely with our estimated ANCP derived from annual nitrate cycles in the euphotic zone. The float-based measurement indicate that the cycle of NCP in the upper ocean and EP are closely balanced, as required to maintain low organic nitrogen stocks in the upper ocean.

Ice edge blooms are a prominent feature of Southern Ocean biogeochemistry [*Smith and Nelson*, 1986]. The largest POC concentrations that were observed by the profiling floats are in the seasonal ice zone (Figure 3). However, the computed ANCP is low in this region, despite relatively large nitrate drawdowns, such as those seen for float 5904472 (Figure 4), which average 5–6 μmol kg^{-1} in the seasonal ice zone. The mixed layers observed by 5904472 are shallow and the vertically integrated annual nitrate drawdown is small compared to that observed by floats further north, such as 5904188 and 5903593 (Figure 4). In the region of the ANCP maximum, mixed layer depths reach several hundred meters with nitrate anomalies around 4 μmol kg^{-1}. The cumulative ANCP is dominated by production in the open waters of the Southern Ocean.

The highest rates of ANCP occur in the region between 40° and 50° South. This is also the region of deepest mixing in the Southern Ocean [*Dong et al*., 2008]. One might expect light limitation driven by deep mixing to produce the lowest ANCP rates in this region. It is possible that dissolved iron supplied by high rates of mixing acts to reduce the chronic iron limitation of the Southern Ocean in this region.

Within the open waters of the Southern Ocean, there is a fundamental difference in the effect of ANCP on atmospheric pCO_2 when it occurs to the north or south of a biogeochemical divide near surface outcrop of the 27.3 kg m^{-3} isopycnal [*Marinov et al*., 2006]. This outcrop is found near 50°S. The distribution of cumulative ANCP (Figure 8) shows that half or more of the ANCP estimated from the seasonal nitrate drawdown in the Southern Ocean occurs to the north of the 27.3 kg m^{-3} isopycnal outcrop, near the maximum in ANCP.

Acknowledgments
This work, including data collection, was sponsored by the US National Science Foundation, Southern Ocean Carbon and Climate Observations and Modeling (SOCCOM) Project under the NSF award PLR-1425989 with additional support from NASA and by the International Argo Program and the NOAA programs that contribute to it. Logistical support for this project in Antarctica was provided by the U.S. National Science Foundation through the U.S. Antarctic Program. Work at MBARI was also supported by the David and Lucile Packard Foundation. We thank all of the people involved in the construction, calibration, and deployment of SOCCOM floats and sensors and the crews of the ships that carried them to sea. All data used in this paper are available at the locations specified in section 3.

References

Arrigo, K. R., D. Worthen, A. Schnell, and M. P. Lizotte (1998), Primary production in Southern Ocean waters, *J. Geophys. Res.*, *103*, 15,587–15,600, doi:10.1029/98JC00930.

Arrigo, K. R., G. L. Van Dijken, and S. Bushinsky (2008), Primary productivity in the Southern Ocean, 1997–2006, *J. Geophys. Res.*, *113*, C08004, doi:10.1029/2007JC004551.

Bender, M. L., and B. Jönsson (2016), Is seasonal net community production in the South Pacific Subtropical Gyre anomalously low?, *Geophys. Res. Lett.*, *43*, 9757–9763, doi:10.1002/2016GL070220.

Boyd, P. W. (2015), Toward quantifying the response of the oceans' biological pump to climate change, *Frontiers Mar. Sci.*, *2*, doi:10.3389/fmars.2015.00077.

Bushinsky, S. M., and S. Emerson (2015), Marine biological production from in situ oxygen measurements on a profiling float in the subarctic Pacific Ocean, *Global Biogeochem. Cycles*, *29*, 2050–2060, doi:10.1002/2015GB005251.

Carr, M.-E., et al. (2006), A comparison of global estimates of marine primary production from ocean color, *Deep Sea Res., Part II*, *53*, 741–770, doi:10.1016/j.dsr2.2006.01.028.

Cetiníc, I., M. J. Perry, N. T. Briggs, E. Kallin, E. A. D'Asaro, and C. M. Lee (2012), Particulate organic carbon and inherent optical properties during 2008 North Atlantic bloom experiment, *J. Geophys. Res.*, *117*, C06028, doi:10.1029/2011JC007771.

Dong, S., J. Sprintall, S. T. Gille, and L. Talley (2008), Southern Ocean mixed-layer depth from Argo profiling floats, *J. Geophys. Res.*, *113*, C06013, doi:10.1029/2006JC004051.

Dunne, J. P., J. L. Sarmiento, and A. Gnanadesikan (2007), A synthesis of global particle export from the surface ocean and cycling through the ocean interior and on the seafloor, *Global Biogeochem. Cycles*, *21*, GB4006, doi:10.1029/2006GB002907.

Dunne, J. P., et al. (2013), GFDL's ESM2 global coupled climate-carbon earth system models. Part II: Carbon system formulation and baseline simulation characteristics, *J. Clim.*, *26*, 2247–2267, doi:10.1175/JCLI-D-12-00150.1.

Emerson, S. (2014), Annual net community production and the biological carbon flux in the ocean, *Global Biogeochem. Cycles*, *28*, 14–28, doi:10.1002/2013GB004680.

Falkowski, P. G., E. A. Laws, R. T. Barber, and J. W. Murray (2003), Phytoplankton and their role in primary, new, and export production, in *Ocean Biogeochemistry, The Role of the Ocean Carbon Cycle in Global Change: A Synthesis of the Joint Global Ocean Flux Study*, edited by M. J. R. Fasham, pp. 99–121, Springer, Berlin.

Gruber, N., C. D. Keeling, and T. F. Stocker (1998), Carbon-13 constraints on the seasonal inorganic carbon budget at the BATS site in the northwestern Sargasso Sea, *Deep Sea Res., Part I*, *45*, 673–717, doi:10.1016/S0967-0637(97)00098-8.

Hansell, D. A., and C. A. Carlson (2001), Biogeochemistry of total organic carbon and nitrogen in the Sargasso Sea: Control by convective overturn, *Deep Sea Res., Part II*, *48*, 1649–1667.

Hennon, T. D., S. C. Riser, and S. Mecking (2016), Profiling float-based observations of net respiration beneath the mixed layer, *Global Biogeochem. Cycles*, *30*, 920–932, doi:10.1002/2016GB005380.

Ito, T., M. Woloszyn, and M. Mazloff (2010), Anthropogenic carbon dioxide transport in the Southern Ocean driven by Ekman flow, *Nature*, *463*, 80–84, doi:10.1038/nature08687.

Johnson, K. S., and H. Claustre (2016), Bringing biogeochemistry into the Argo age, *Eos Trans. AGU*, *97*, doi:10.1029/2016EO062427.

Johnson, K. S., and L. J. Coletti (2002), In situ ultraviolet spectrophotometry for high resolution and long term monitoring of nitrate, bromide and bisulfide in the ocean, *Deep Sea Res., Part I*, *49*, 1291–1305, doi:10.1016/S0967-0637(02)00020-1.

Johnson, K. S., S. C. Riser, and D. M. Karl (2010), Nitrate supply from deep to near-surface waters of the North Pacific subtropical gyre, *Nature*, *465*, 1062–1065, doi:10.1038/nature09170.

Johnson, K. S., L. Coletti, H. Jannasch, C. Sakamoto, D. Swift, and S. Riser (2013), Long-term nitrate measurements in the ocean using the in situ ultraviolet spectrophotometer: Sensor integration into the Apex profiling float, *J. Atmos. Oceanic Technol.*, *30*, 1854–1866, doi:10.1175/JTECH-D-12-00221.1.

Johnson, K. S., O. Pasqueron de Fommervault, R. Serra, F. D'Ortenzio, C. Schmechtig, H. Claustre, and A. Poteau (2016), *Processing Bio-Argo Nitrate Concentration at the DAC Level, v1.0*, doi:10.13155/46121.

Johnson, et al. (2017), Biogeochemical sensor performance in the SOCCOM profiling float array, *J. Geophys. Res. Oceans*, *122*, doi:10.1002/2017JC012838.

Karl, D. M., et al. (2003), Temporal studies of biogeochemical processes determined from ocean time-series observations during the JGOFS era, in *Ocean Biogeochemistry, The Role of the Ocean Carbon Cycle in Global Change: A Synthesis of the Joint Global Ocean Flux Study*, edited by M. J. R. Fasham, pp. 239–267, Springer, Berlin.

Keeling, C., H. Brix, and N. Gruber (2004), Seasonal and long-term dynamics of the upper ocean carbon cycle at station ALOHA near Hawaii, *Global Biogeochem. Cycles*, *18*, GB4006, doi:10.1029/2004GB002227.

Knapp, A. N., D. M. Sigman, and F. Lipschultz (2005), N isotopic composition of dissolved organic nitrogen and nitrate at the Bermuda Atlantic Time-series Study site, *Global Biogeochem. Cycles*, *19*, GB1018, doi:10.1029/2004GB002320.

Landschützer, P., et al. (2015), The reinvigoration of the Southern Ocean carbon sink, *Science*, *349*(6253), 1221–1224, doi:10.1126/science.aab2620.

Laws, E. A., P. G. Falkowski, W. O. Smith Jr., H. W. Ducklow, and J. J. McCarthy (2000), Temperature effects on export production in the open ocean, *Global Biogeochem. Cycles*, *14*, 1231–1246, doi:10.1029/1999GB001229.

Laws, E. A., E. D'Sa, and B. Naik (2011), Simple equations to estimate ratios of new or export production to total production from satellite derived estimates of sea surface temperature and primary production, *Limnol. Oceanogr. Methods*, *9*, 593–601, doi:10.4319/lom.2011.9.593.

Lee, K. (2001), Global net community production estimated from the annual cycle of surface water total dissolved inorganic carbon, *Limnol. Oceanogr.*, *46*, 1287–1297, doi:10.4319/lo.2001.46.6.1287.

Letelier, R. M., D. M. Karl, M. R. Abbott, and R. R. Bidigare (2004), Light driven seasonal patterns of chlorophyll and nitrate in the lower euphotic zone of the North Pacific Subtropical Gyre, *Limnol. Oceanogr.*, *49*(2), 508–519, doi:10.4319/lo.2004.49.2.0508.

Leung, S., A. Cabre, and I. Marinov (2015), A latitudinally banded phytoplankton response to 21st century climate change in the Southern Ocean across the CMIP5 model suite, *Biogeoscience*, *12*, 5715–5734, doi:10.5194/bg-12-5715-2015.

Lipschultz, F. (2001), A time-series assessment of the nitrogen cycle at BATS, *Deep Sea Res., Part II*, *48*, 1897–1924, doi:10.1016/S0967-0645(00)00168-5.

Lourey, M. J., and T. W. Trull (2001), Seasonal nutrient depletion and carbon export in the Subantarctic and Polar Frontal zones of the Southern Ocean south of Australia, *J. Geophys. Res.*, *106*, 31,463–31,487, doi:10.1029/2000JC000287.

MacCready, P., and P. Quay (2001), Biological export flux in the Southern Ocean estimated from a climatological nitrate budget, *Deep Sea Res., Part II*, *48*, 4299–4322, doi:10.1016/S0967-0645(01)00090-X.
MacIntyre, G., B. Plache, M. R. Lewis, J. Andrea, S. Feener, S. D. McLean, K. S. Johnson, L. J. Coletti, and H. W. Jannasch (2009), ISUS/SUNA nitrate measurements in networked ocean observing systems, in *OCEANS 2009, MTS/IEEE Biloxi-Marine Technology for Our Future: Global and Local Challenges*, pp. 1–7, Inst. of Electr. and Electr. Eng.
MacKenzie, L., I. Sims, V. Beuzenberg, and P. Gillespie (2002), Mass accumulation of mucilage caused by dinoflagellate polysaccharide exudates in Tasman Bay, New Zealand, *Harmful Algae*, *1*, 69–83, doi:10.1016/S1568-9883(02)00006-9.
Marinov, I., A. Gnanadesikan, J. R. Toggweiler, and J. L. Sarmiento (2006), The Southern Ocean biogeochemical divide, *Nature*, *441*, 964–967, doi:10.1038/nature04883.
Marinov, I., A. Gnanadesikan, J. L. Sarmiento, J. R. Toggweiler, M. Follows, and B. K. Mignone (2008), Impact of oceanic circulation on biological carbon storage in the ocean and atmospheric pCO2, *Global Biogeochem. Cycles*, *22*, GB3007, doi:10.1029/2007GB002958.
Martz, T. R., K. S. Johnson, and S. C. Riser, (2008), Ocean metabolism observed with oxygen sensors on profiling floats in the Pacific, *Limnol. Oceanogr.*, *53*, 2094–2111, doi:10.4319/lo.2008.53.5_part_2.2094.
McNeil, B. J., and B. Tilbrook, (2009), A seasonal carbon budget for the sub-Antarctic Ocean, south of Australia, *Mar. Chem.*, *115*, 196–210, doi:10.1016/j.marchem.2009.08.006.
Michaels, A. F., N. R. Bates, K. O. Buesseler, C. A. Carlson, and A. H. Knap (1994), Carbon-cycle imbalances in the Sargasso Sea, *Nature*, *372*, 537–540, doi:10.1038/372537a0.
Moore, J. K., and M. R. Abbott (2000), Phytoplankton chlorophyll distributions and primary production in the Southern Ocean, *J. Geophys. Res.*, *105*, 28,709–28,722, doi:10.1029/1999JC000043.
Moore, J. K., M. R. Abbott, and J. G. Richman (1999), Location and dynamics of the Antarctic Polar Front from satellite sea surface temperature data, *J. Geophys. Res.*, *104*, 3059–3073, doi:10.1029/1998JC900032.
Munro, D., N. Lovenduski, B. Stephens, T. Newberger, K. Arrigo, T. Takahashi, P. Quay, J. Sprintall, N. Freeman, and C. Sweeney (2015), Estimates of net community production in the Southern Ocean determined from time series observations (2002–2011) of nutrients, dissolved inorganic carbon, and surface ocean pCO_2 in Drake Passage, *Deep Sea Res., Part II*, *114*, 49–63, doi:10.1016/j.dsr2.2014.12.014.
Nevison, C. D., R. F. Keeling, M. Kahru, M. Manizza, B. G. Mitchell, and N. Cassar (2012), Estimating net community production in the Southern Ocean based on atmospheric potential oxygen and satellite ocean color data, *Global Biogeochem. Cycles*, *26*, GB1020, doi:10.1029/2011GB004040.
Nicholson, D., S. Emerson, and C. C. Eriksen (2008), Net community production in the deep euphotic zone of the subtropical North Pacific gyre from glider surveys, *Limnol. Oceanogr.*, *53*(5_part_2), 2226–2236, doi:10.4319/lo.2008.53.5_part_2.2226.
Olsen, A., et al. (2016), The Global Ocean Data Analysis Project version 2 (GLODAPv2)—An internally consistent data product for the world ocean, *Earth Syst. Sci. Data*, *8*, 297–323, doi:10.5194/essd-8-297-2016.
Orsi, A. H., T. Whitworth III, and W. D. Nowlin Jr. (1995), On the meridional extent and fronts of the Antarctic Circumpolar Current, *Deep Sea Res., Part I*, *42*, 641–673, doi:10.1016/0967-0637(95)00021-W.
Parekh, P., S. Dutkiewicz, M. J. Follows, and T. Ito (2006), Atmospheric carbon dioxide in a less dusty world, *Geophys. Res. Lett.*, *33*, L03610, doi:10.1029/2005GL025098.
Pasqueron de Fommervault, O., et al. (2015), Seasonal variability of nutrient concentrations in the Mediterranean Sea: Contribution of Bio-Argo floats, *J. Geophys. Res. Oceans*, *120*, 8528–8550, doi:10.1002/2015JC011103.
Plant, J. N., K. S. Johnson, C. M. Sakamoto, H. W. Jannasch, L. J. Coletti, S. C. Riser, and D. D. Swift (2016), Net community production at Ocean Station Papa observed with nitrate and oxygen sensors on profiling floats, *Global Biogeochem. Cycles*, *30*, 859–879, doi:10.1002/2015GB005349.
Pollard, R., P. Tréguer, and J. Read (2006), Quantifying nutrient supply to the Southern Ocean, *J. Geophys. Res.*, *111*, C05011, doi:10.1029/2005JC003076.
Riebesell, U., A. Kortzinger, and A. Oschlies (2009), Sensitivities of marine carbon fluxes to ocean change, *Proc. Natl. Acad. Sci. U. S. A.*, *106*(49), 20,602–20,609, doi:10.1073/pnas.0813291106.
Riser, S. C., and K. S. Johnson (2008), Net production of oxygen in the subtropical ocean, *Nature*, *451*, 323–325, doi:10.1038/nature06441.
Riser, S. C., et al. (2016), Fifteen years of ocean observations with the global Argo array, *Nat. Clim. Change*, *6*, 145–153, doi:10.1038/nclimate2872.
Rudnick, D. L. (2016), Ocean research enabled by underwater gliders, *Annu. Rev. Mar. Sci.*, *8*, 519–541, doi:10.1146/annurev-marine-122414-033913.
Rudnick, D. L., R. Baltes, M. Crowley, C. M. Lee, C. Lembke, and O. Schofield (2012), A national glider network for sustained observation of the coastal ocean, in *IEEE Oceans 2012*, doi:10.1109/OCEANS.2012.6404956.
Sarmiento, J. L., A. Gnanadesikan, I. Marinov, and R. D. Slater (2011), The role of marine biota in the CO_2 balance of the ocean-atmosphere system, in *The Role of Marine Biota in the Functioning of the Biosphere*, edited by C. M. Duarte, pp. 71–105, Fundación BBVA, Bilbao.
Sauzède, R., H. Claustre, O. Pasqueron de Fommervault, H. Bittig, J.-P. Gattuso, L. Legendre, and K. S. Johnson (2017), Global estimates of water column nutrients concentration and carbonate system parameters in the Ocean: A novel approach based on neural networks, *Frontiers Mar. Sci.*, *4*, 128, doi:10.3389/fmars.2017.00128.
Schlitzer, R. (2000), Applying the adjoint method for biogeochemical modeling: Export of particulate organic matter in the world ocean, in *Inverse Methods in Global Biogeochemical Cycles*, edited by P. Kasibhatla et al., pp. 107–124, AGU, Washington, D. C., doi:10.1029/GM114p0107.
Schlitzer, R. (2002), Carbon export fluxes in the Southern Ocean: Results from inverse modeling and comparison with satellite-based estimates, *Deep Sea Res., Part II*, *49*, 1623–1644, doi:10.1016/S0967-0645(02)00004-8.
Schmechtig, C., A. Poteau, H. Claustre, F. D'Ortenzio, G. Dall'Olmo, and E. Boss (2016), *Processing Bio-Argo Particle Backscattering at the DAC Level*, doi:10.13155/39459.
Shadwick, E. H., T. W. Trull, B. Tilbrook, A. J. Sutton, E. Schulz, and C. L. Sabine (2015), Seasonality of biological and physical controls on surface ocean CO_2 from hourly observations at the Southern Ocean Time Series site south of Australia, *Global Biogeochem. Cycles*, *29*, 223–238, doi:10.1002/2014GB004906.
Shang, S. L., M. J. Behrenfeld, Z. P. Lee, R. T. O'Malley, G. M. Wei, Y. H. Li, and T. Westberry (2010), Comparison of primary production models in the Southern Ocean—Preliminary results, in *Proc. SPIE 7678, Ocean Sensing and Monitoring II*, edited by W. Hou and R. Arnone, doi:10.1117/12.853631.
Smith, W. O., and D. M. Nelson (1986), Importance of ice edge phytoplankton blooms in the Southern Ocean, *Bioscience*, *36*, 251–257.
Stephenson, G. R., Jr., S. T. Gille, and J. Sprintall (2012), Seasonal variability of upper ocean heat content in Drake Passage, *J. Geophys. Res.*, *117*, C04019, doi:10.1029/2011JC007772.

Wang, X., R. J. Matear, and T. W. Trull (2003), Nutrient utilization ratios in the Polar Frontal Zone in the Australian sector of the Southern Ocean: A model, *Global Biogeochem. Cycles*, *17*(1), 1009, doi:10.1029/2002GB001938.

Watson, A. J., and J. C. Orr (2003), Carbon dioxide fluxes in the global ocean, in *Ocean Biogeochemistry, The Role of the Ocean Carbon Cycle in Global Change: A Synthesis of the Joint Global Ocean Flux Study*, edited by M. J. R. Fasham, pp. 123–141, Springer, Berlin.

Williams, N. L., R. A. Feely, C. L. Sabine, A. G. Dickson, J. H. Swift, L. D. Talley, and J. L. Russell (2015), Quantifying anthropogenic carbon inventory changes in the Pacific sector of the Southern Ocean, *Mar. Chem.*, *174*, 147–160, doi:10.1016/j.marchem.2015.06.015.

Williams, N. L., L. W. Juranek, K. S. Johnson, R. A. Feely, S. C. Riser, L. D. Talley, J. L. Russell, J. L. Sarmiento, and R. Wanninkhof (2016), Empirical algorithms to estimate water column pH in the Southern Ocean, *Geophys. Res. Lett.*, *43*, 3415–3422, doi:10.1002/2016GL068539.